REPORT DOCUMENTATION PAGE

Form Approved
OMB No. 0704-0188

maintaining the data needed, and completing and reviewing this collection of information. Send comments regarding this burden estimate or any other aspect of this collection of information, including suggestions for reducing this burden to Department of Defense, Washington Headquarters Services, Directorate for Information Operations and Reports (0704-0188), 1215 Jefferson Davis Highway, Suite 1204, Arlington, VA 22202-4302. Respondents should be aware that notwithstanding any other provision of law, no person shall be subject to any penalty for failing to comply with a collection of information if it does not display a currently valid OMB control number. **PLEASE DO NOT RETURN YOUR FORM TO THE ABOVE ADDRESS.**

1. REPORT DATE *(DD-MM-YYYY)*	2. REPORT TYPE	3. DATES COVERED *(From - To)*
May 2002	Conference Proceedings	5/01 - 5/02

4. TITLE AND SUBTITLE
Advanced Optical Diagnostics for HF Laser Development

5a. CONTRACT NUMBER
F29601-01-C-0091

5b. GRANT NUMBER

5c. PROGRAM ELEMENT NUMBER
65502F

6. AUTHOR(S)
W. T. Rawlins, D. B. Oakes, P. A. Mulhall, S. J. Davis, R. F. Wright, D. L. Carroll, and L. H. Sentman

5d. PROJECT NUMBER

5e. TASK NUMBER

5f. WORK UNIT NUMBER
3005DOFN

7. PERFORMING ORGANIZATION NAME(S) AND ADDRESS(ES)

Physical Sciences, Inc.
20 New England Business Center
Andover, MA 01810

8. PERFORMING ORGANIZATION REPORT NUMBER

9. SPONSORING / MONITORING AGENCY NAME(S) AND ADDRESS(ES)
Gerald C. Manke II
Air Force Research Laboratory
Directed Energy Directorate
3550 Aberdeen Ave. SE
Kirtland AFB, NM 87117

10. SPONSOR/MONITOR'S ACRONYM(S)

11. SPONSOR/MONITOR'S REPORT NUMBER(S)

12. DISTRIBUTION / AVAILABILITY STATEMENT
Approved for public release; distribution is unlimited

13. SUPPLEMENTARY NOTES
Proceedings of the 33rd AIAA Plasmadynamics and Lasers Conference
AIAA-2002-2221

14. ABSTRACT

We present results from a study that used a non-intrusive diagnostic for mixing, species concentration, optical gain, and spatial beam profile for HF chemical lasers. The instrument is based on hyperspectral imaging using a low order Fabry-Perot interferometer. The basic theory behind this technology is described and several applications to a chemically reacting flow field are presented. We also discuss application of this device to a subsonic HF chemical laser.

20020905 070

15. SUBJECT TERMS
HF chemical lasers, chemical laser diagnostics, hyperspectral imaging, reactive flows

16. SECURITY CLASSIFICATION OF:			17. LIMITATION OF ABSTRACT	18. NUMBER OF PAGES	19a. NAME OF RESPONSIBLE PERSON
a. REPORT	b. ABSTRACT	c. THIS PAGE	Unlimited	9	Gerald C. Manke II
Unclassified	Unclassified	Unclassified			19b. TELEPHONE NUMBER *(include area code)* 505-853-2674

AIAA 2002-2221
Advanced Optical Diagnostics for HF Laser Development

W.T. Rawlins, D.B. Oakes, P.A. Mulhall, and S.J. Davis
Physical Sciences Inc.
20 New England Business Center
Andover, MA 01810

R.F. Wright, D.L. Carroll, and L.H. Sentman
Aeronautical and Astronautical Engineering Department
University of Illinois
Urbana, IL 61801

AIAA Conference:
33rd Plasmadynamics and Lasers
May 2002/Maui, HI

For permission to copy or republish, contact the copyright owner named on the first page.
For AIAA-held copyright, write to AIAA Permissions Department,
1801 Alexander Bell Drive, Suite 500, Reston, VA 20191-4344.

Copyright © 2002 by the American Institute of Aeronautics and Astronautics, Inc. All rights reserved.

AIAA-2002-2221

ADVANDED OPTICAL DIAGNOSTICS FOR HF LASER DEVELOPMENT

W.T. Rawlins*, D.B. Oakes*, P.A. Mulhall† and S.J. Davis‡
Physical Sciences Inc.
Andover, MA 01810

R.F. Wright§, D.L. Carroll¶, and L.H. Sentman¶
Aeronautical and Astronautical Engineering Department
University of Illinois
Urbana, IL 61801

Abstract

We present results from a study that used a non-intrusive diagnostic for mixing, species concentration, optical gain, and spatial beam profile for HF chemical lasers. The instrument is based on hyperspectral imaging using a low order Fabry-Perot interferometer. The basic theory behind this technology is described and several applications to a chemically reacting flow-field are presented. We also discuss application of this device to a subsonic, HF chemical laser.

Introduction

It is well known that certain gas phase chemical reactions form product states that have inverted population distributions. For example, the F + H_2 reaction produces H + HF(v,J) where partial inversions exist between many rovibrational levels. Mixing of the reacting gas streams in a chemical laser is a key parameter for producing efficient devices.[1-3] This was recognized soon after the first laser demonstrations, but effective diagnostics did not exist that could survive corrosive environments or did not perturb the flows. Measurements of mixing, vibrational and rotational temperatures, small signal gain, and spectral output were difficult and often inaccurate. Even though the HF chemical laser concept is more than 30 years old, there are still important scaling parameters for which there are no effective diagnostics. In 1978 Rapagnani and Davis demonstrated that laser induced fluorescence could be used as a diagnostic for mixing in chemical laser nozzles, and they later developed methods for studying both hot flow and cold flow mixing.[4,5] In this paper we discuss a new diagnostic for reactive mixing in chemical lasers. Using a device we call the Adaptive Infrared Imaging Spectroradiometer (AIRIS) we have developed methods for examining mixing of F and H_2 flows and for determining spatially resolved maps of population inversions between selected HF rovibrational levels. In addition, we provide examples of spatially and spectrally resolved output beam profiles recorded using this hyperspectral imaging device.

Background

The AIRIS technology was developed at Physical Sciences Inc. (PSI) to address the need for a moderate resolution, rapidly tuned imaging spectrometer for a variety of applications. Our technology is based on Fabry-Perot (F-P) interferometry. Fabry-Perot devices rely upon multiple beam interference between two highly reflecting mirrors to produce an interference pattern that contains spectral information about the light source being probed. If the light source is collimated with a lens, then the resulting interference pattern is usually a series of concentric rings, each representing a different order of the interference. This is illustrated in Figure 1.

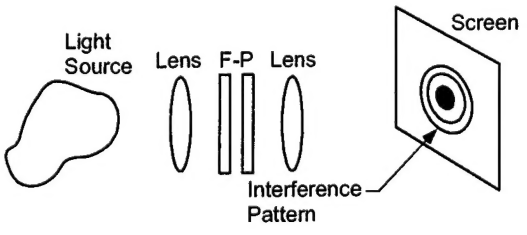

Figure 1. Typical arrangement for F-P interferometers.

*Principal Research Scientist
†Instrumentation Specialist
‡Principal Research Scientist, Member AIAA
sdavis@psicorp; phone 1.978.0003; fax 1.978.3232; http://www.psicorp.com; Physical Sciences Inc., 20 New England Business Center, Andover, MA USA 01810-1077
§Graduate Student, Member AIAA
¶Professor, Member AIAA
Copyright © 2002 by Physical Sciences Inc. Published by the American Institute of Aeronautics and Astronautics, Inc. with permission.

Jacquinot[6] described an important application of the F-P with the introduction of the center spot technique. He showed that if one placed a pinhole in front of a detector that restricted the detector to view only a small portion of the center spot of the interference pattern, then one could use the F-P as a spectrometer by recording the transmitted light as a function of the distance between the F-P mirrors. Davis and co-workers[7] used this approach to obtain the first measurements of the collisional broadening coefficient for oxygen on the atomic iodine laser line, crucial data for COIL. This type of spectrometer offers several advantages including: high throughput, high spectral resolution, and compact size.

Basic Concepts

The *AIRIS* instrument comprises an IR focal plane array (FPA) coupled to a Fabry-Perot interferometer through imaging optics. In this configuration the interferometer operates as a tunable interference filter, selecting the wavelength viewed by the FPA. In this section we describe the theoretical basis for the development of the interferometer as well as the consequences and advantages of low-order operation.

In a Fabry-Perot interferometer light is selectively transmitted by constructive interference through the faces of two partially-reflecting parallel mirrors. Light is transmitted for wavelengths which satisfy the expression:

$$\lambda_t = \frac{2\ell}{m}\cos\theta \qquad (1)$$

where

ℓ = mirror spacing
m = order of interference
θ = incidence angle
λ_t = transmitted wavelength.

A range of mirror spacings, incidence angles, and orders will all lead to the transmission of a single wavelength. The free spectral range, $\Delta\lambda_{FSR}$, determines the range of wavelengths transmitted between successive orders of interference:

$$\Delta\lambda_{FSR} = \frac{\lambda_{max}}{m_{max}+1} \qquad (2)$$

where m_{max} is the order in which λ_{max} is transmitted for paraxial rays.

The finesse, F, determines the spectral resolution of the interferometer, which is always a fraction of the free spectral range:

$$\Delta\lambda_{1/2} = \frac{\Delta\lambda_{FSR}}{F} \qquad (3)$$

The elements which define the finesse of the interferometer arise from the reflectivities of the mirrors as well as "defects" in their configuration, such as mirror flatness and parallelism. The total finesse of the interferometer is obtained from the inverse root mean square sum of each finesse component. For practical operation in the infrared, the defect finesse is the limiting factor in determining total finesse. The total finesse can seldom be greater than approximately 30 to 50 due to these limitations.

The interferometer field of view (focal length and detector element size) determines the range of angles incident and detected by the system. Equation (1) shows that a range of incidence angles and interference orders will allow transmission of a common wavelength through the interferometer for a single mirror spacing. The aperture finesse defines the degradation in spectral resolution within a single order due to this effect:

$$F_A = \frac{2}{m(\Delta\theta)^2} \qquad (4)$$

As a consequence of Eq. (4), the field of view over which an acceptable finesse can be obtained increases as the interferometer is operated in lower orders. When using IR focal plane arrays, system instantaneous fields-of-view ranging from 6 to 15 deg are generally consistent with an overall finesse of 35.

The short wavelength AIRIS used in this work contains two, custom mirrors with high reflectivity in the 2.0 to 3 micron spectral region. The 38 mm diameter mirrors were fitted with specialized gold pads that form four capacitors that are used to measure and monitor the separation and alignment of the two mirrors in the Fabry-Perot configuration. A photo of the short wavelength AIRIS head is shown in Figure 2.

Figure 2. Photo of AIRIS device used to probe HF(v,J) emission.

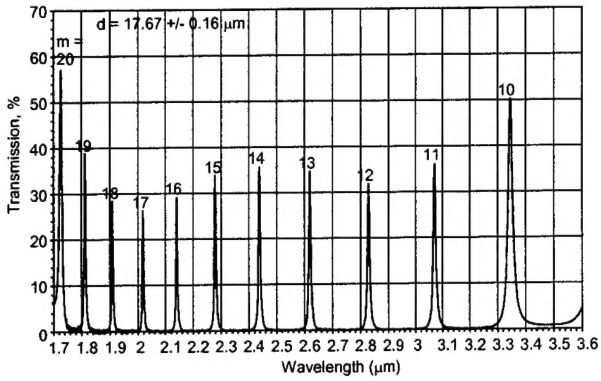

Figure 3. AIRIS transmission as a function of the wavelength of incident light for a mirror separation of 17.67 ± 0.16 μm. The interference order is also indicated. Spectral resolution is 2 cm^{-1}.

Experiments

Calibrations

Initial testing of the AIRIS system was conducted using a Fourier Transform Infrared (FTIR) spectrometer. The AIRIS head was positioned inside the FTIR, and the FTIR provides a tunable, narrow spectral band of light that can be used as an essentially monochromatic source for AIRIS calibrations. This quasi-monochromatic beam (0.5 to 2 cm^{-1}) passed through the AIRIS and the transmitted intensity was monitored as a function of the wavelength of the source and the mirror separation in AIRIS. Recall that in a Fabry-Perot interferometer the wavelength of the transmitted light is a function of the mirror separation. We performed initial calibration of the AIRIS by systematically setting the mirror separation while recording the transmitted intensity as the wavelength of the light passed by the FTIR was scanned. As the wavelength of the light incident on the AIRIS passed through cavity resonances, transmission peaks of the consecutive orders were observed. A typical spectrum is shown in Figure 3.

Chemical HF (v,J) Production

We used a high power Microwave Driven Jet (MIDJet™) device to produce the F atoms. MIDJet™ is an electrodeless discharge so that corrosion is not an issue. It has been applied to numerous feedstock gases including SF_6, O_2, He, Cl_2, NF_3, and air. The source gas and diluent are fed into the discharge region of MIDJet™ through a series of sonic injection nozzles. The design of these injectors stabilizes the discharge along the axis of the MIDJet™ chamber and enables the device to operate over a large range of pressures and flow rates. Both sonic and subsonic exit nozzles can be used to cover a wide range of exit conditions. The supersonic exit nozzle isolates the conditions inside the MIDJet™ chamber for flow conditions downstream of the nozzle.

The injector was mounted in the MIDJet™ source as indicated in Figure 4. The HF mixing nozzle for production of HF(v,J) from the F + H_2 reaction was a 6 mm diameter stainless tube with four holes (0.5 mm diameter) spaced 1.5 cm apart. Hydrogen and He dilutent were injected through this arrangement. The four holes produced supersonic flows of H_2 from the exit plane to approximately 2 mm downstream of the holes. Fluorine atoms were produced with a 5 kW MIDJet™ discharge device using SF_6 as the feedstock gas. Details of the water-cooled injector tube are shown in Figure 5.

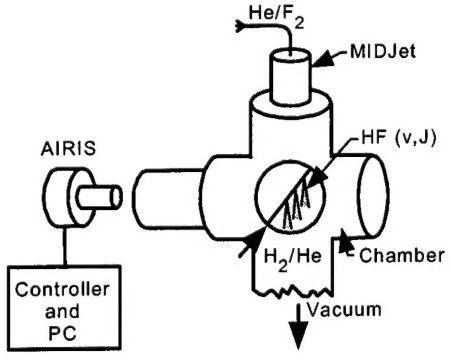

Figure 4. Block diagram showing injector mounted in MIDJet™ device.

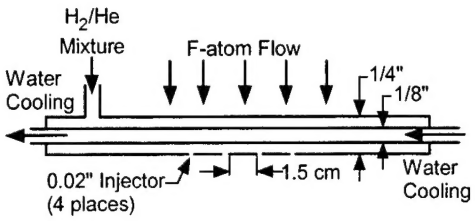

Figure 5. H_2 injector used in the MIDJet™, HF production chamber.

Tests of AIRIS on HF Flow Chamber

The AIRIS device was positioned in front of a Cincinnati Electronics InSb IR camera equipped with a 4.1 μm short-pass cold filter. We also used a bandpass filter to isolate the emission in the 2.6 to 2.9 μm spectral region. The filter was placed directly in front of the camera. A camera zoom lens was used to focus the region of the HF injector, with the camera approximately 60 cm from the HF injector. In order to assure that the HF production chemistry made HF(v,J) we initially viewed the reaction zone with the FTIR spectrometer. The spectral region recorded between 2.65 and 2.9 μm is shown in Figure 6. Each feature can be assigned to an HF emission line and no other spectral features were observed. Even though the spectra are uncorrected for spectral response, it appears that the vibrational distribution is inverted with v=2 having more population than v=1. Our source of HF appears to be an excellent surrogate for an actual HF laser reaction zone.

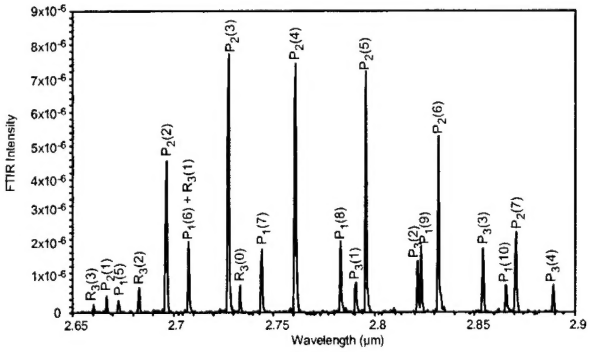

Figure 6. FTIR spectrum of HF(v,J) emission recorded in our HF production chamber. Spectral resolution is 0.5 cm^{-1}.

Figure 7 shows an image of the HF flowfield obtained with the AIRIS. The image is emission from the $P_2(4)$ line near 2.76 μm. The mixing of the F and H_2 downstream of the injection points is clearly evident. When the AIRIS is tuned off the $P_2(4)$ line (near the $P_1(7)$ line), the emission disappears, demonstrating the ability of AIRIS to spectrally isolate the HF emission lines. We have collected emission from numerous lines. Each image was also complemented by recording a full field image of a flat blackbody radiator at each wavelength. This allowed us to subsequently put each image on an absolute intensity basis. We also recorded a background image with the H_2 flow off. The raw images were corrected using the following procedure. First a background image was subtracted from each "raw" image. To correct each pixel for spectral response, each image was divided by the blackbody function at the appropriate wavelength of the image.

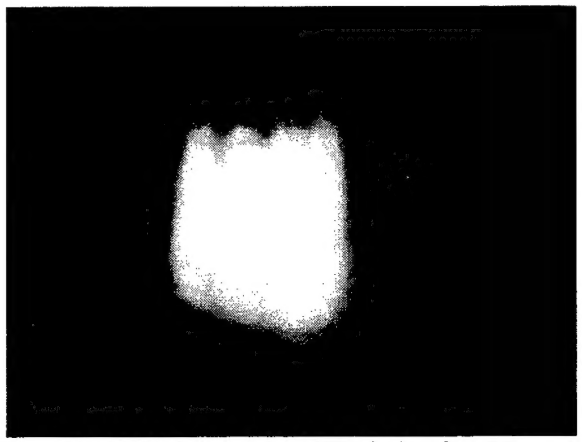

Figure 7. AIRIS image of $P_2(4)$ emission from chemically produced HF.

To further demonstrate that AIRIS can be used to study mixing phenomena in an HF laser, we performed an additional analysis on the flow field images. In Figure 8 we show a section of the mixing region just downstream of the hydrogen injectors. Four planes: A, B, C, and D are shown. In Figure 9 we show contours of these four planes and the progression of the mixing is evident as the flow progresses from A to D.

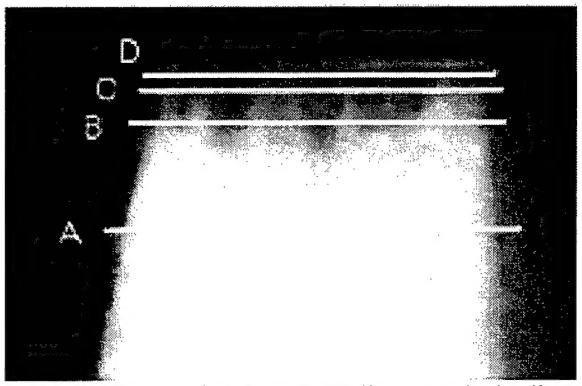

Figure 8. HF emission from $P_2(5)$ line. Analysis slices are indicated. Flow direction is down.

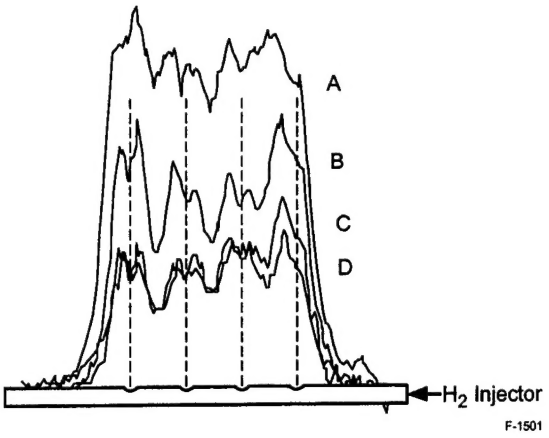

Figure 9. Intensity profiles from image shown in Figure 8. Flow direction is up.

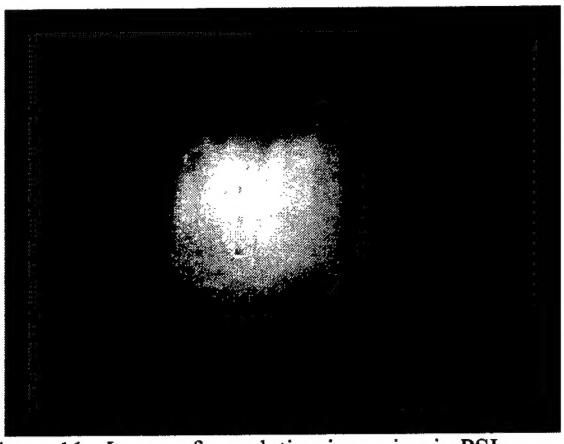

Figure 11. Image of population inversion in PSI flowfield.

We also developed a strategy to image the population inversion in the flowfield. When placed on an absolute scale, one can subtract images of the same scene recorded on sequential emission transitions to obtain these population inversion images. The method is outlined in Figure 10. We used this approach to produce images of the inversion density of the flow field. Figure 11 shows an image of the spatially resolved population inversion between the HF(v,J) = (2,4) and (1,5) levels. This key demonstration shows that AIRIS can be used to interrogate the small signal gain, a key parameter in HF lasers.

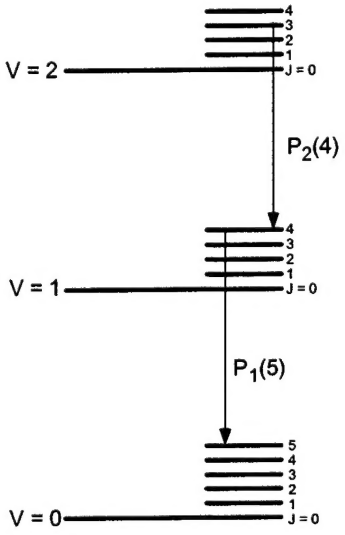

Figure 10. Strategy for obtaining images of population inversion fields.

We also completed a field test of the AIRIS device at the University of Illinois, Urbana Champaign (UIUC) supersonic HF laser. A diagram of the optical measurement setup is shown in Figure 12. The UIUC supersonic laser (SSL) operates via supersonic injection of H_2 into a supersonic flow of effluent from an electric discharge of $SF_6/O_2/He$ mixtures. The H_2 is injected through a bank of nozzles to produce a mixing region some 30 cm long, in which atomic F from the discharge reacts with H_2 to form rovibrationally excited HF(v,J). This reaction results in intense chemiluminescent emission from the excited states of HF(v = 1 to 3, J = 1 to 15) in the 2.3 to 3.2 μm spectral region. Upon application of a mirror and a partially reflecting output coupler, the reaction zone immediately downstream of the nozzle bank forms a laser cavity, with gain on several P-branch transitions from the v' = 1 and 2 vibrational levels. The AIRIS tests employed two different out-couplers, one 50% reflective and one 73% reflective, in order to compare the observed spectral content, beam shapes, and temporal stability. For both out-couplers, the observed beam dimensions were ~0.5 cm vertical and ~1.0 cm horizontal. The observed power levels were 30 W for the 50% out-coupler and 50 W for the 73% out-coupler.

As shown in the diagram, the laser output beam was passed through a curved (R = 2 m), 93% reflective mirror, which served as a beamsplitter to reduce the projected laser intensity. This mirror also expanded the transmitted beam, which was reflected by a plane gold mirror onto a screen some 4 m away. The resulting magnification of the projected beam was a factor of ~5 at the screen. The total power on the screen was ~2 W

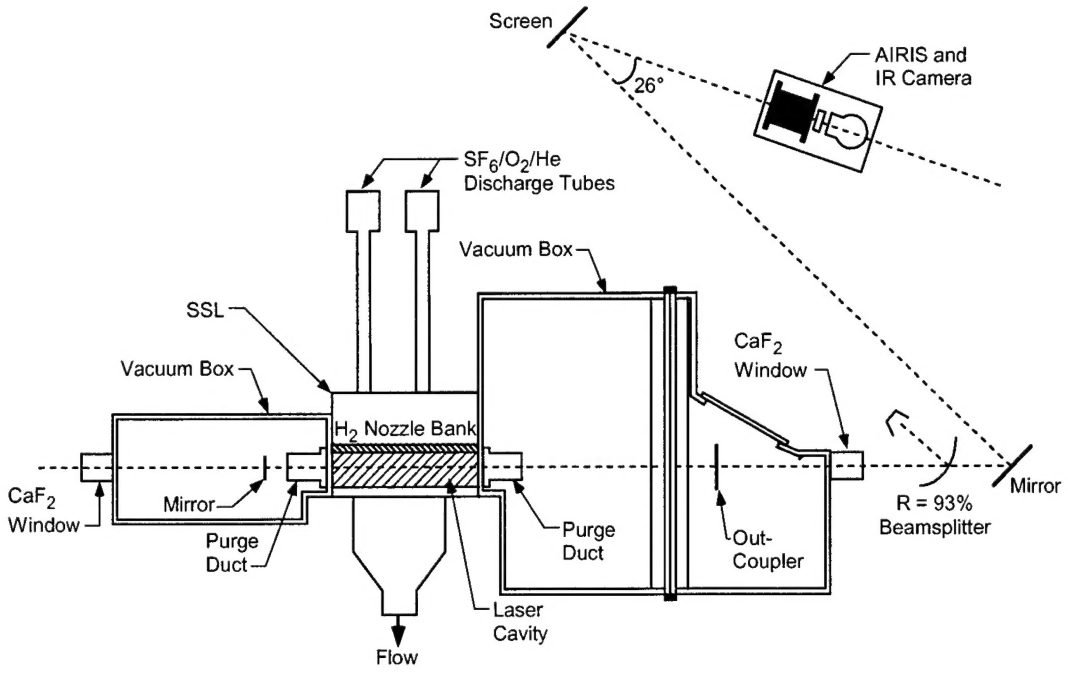

Figure 12. Optical setup for AIRIS spectral imaging measurements of projected SSL laser beam at UIUC.

for the 50% out-coupler and ~3.5 W for the 73% out-coupler.

The AIRIS detection system was mounted on a tripod and viewed the projected beam at an angle of 26 deg, from a distance of ~1.3 m. The observed radiation passed through the AIRIS filter, through a 2.65 to 2.90 μm order-sorting bandpass filter, through a 50 mm lens, and into the Cincinnati Electronics infrared camera. The InSb focal plane array measures 120 (vertical) by 160 (horizontal) pixels; each pixel is 50 μm square. The camera is cooled by liquid nitrogen and contains a 4.1 μm short-pass cold filter to reduce noise from room-temperature thermal radiation. The measured magnification factor of the lens is 1:24.5, resulting in a single-pixel spatial resolution of 0.12 cm and a field of regard 14.7 cm vertical x 19.6 cm horizontal.

Spectral images were recorded by both computerized frame acquisition and video recording for a variety of wavelengths and laser operating conditions. Images were recorded for both out-couplers. The AIRIS spectral scans confirmed that the observed lasing transitions were $P_1(6\text{-}9)$ and $P_2(6\text{-}8)$ for the 50% out-coupler, and $P_1(7\text{-}9)$ and $P_2(6\text{-}9)$ for the 73% out-coupler. Example spectral images comparing the projected beam for the two out-couplers are shown in Figures 13 and 14. The figures show false color encoded images of the beam profiles for the cascade pair $P_1(8)$ and $P_2(7)$, for the 50% (Figure 13) and 73% (Figure 14) out-couplers.

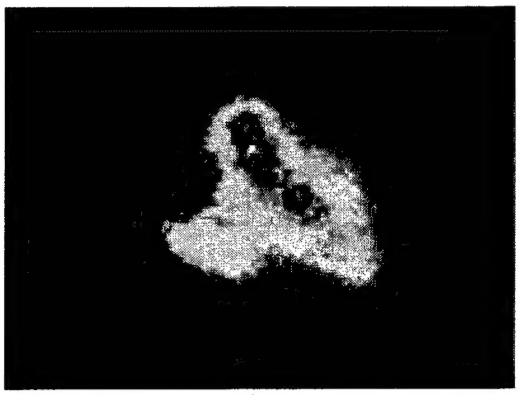

(a)

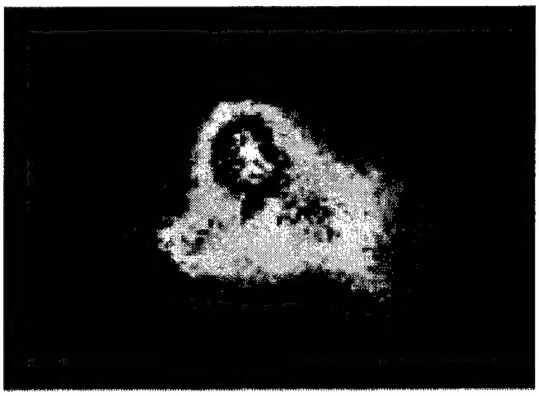

(b)

Figure 13. ARIS spectral images of projected SSL intensities of (a) $P_1(8)$ and (b) $P_2(7)$ laser lines for the 50% out-coupler at 30 W output power.

(a)

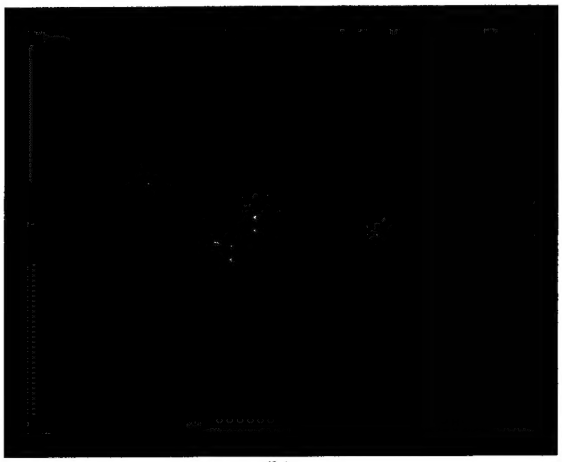

(b)

Figure 14. AIRIS spectral images of projected SSL intensities of (a) $P_1(8)$ and (b) $P_2(7)$ laser lines for the 73% out-coupler at 50 W total power.

The images are corrected for background radiation and for spectral responsivity, resulting in a gray scale proportional to the absolute radiance in W/(cm^2 sr μm). Additional spectral scans were performed to characterize the instrument's spectral resolution and out-of-band rejection. The observed temporal behavior of the projected beam for the 73% out-coupler was recorded at several wavelengths by video tape. The observed temporal fluctuations included a fast, single-pixel-sized scintillation which may have been caused by small density fluctuations along the beam path, laser speckle, or occasional flickering in the overall beam.

Summary

We have described a novel diagnostic capable of probing chemically reacting flows for species concentration maps, mixing, and even population inversion maps. Using a subsonic flow reactor, we have obtained spatially and spectrally resolved maps of emission from excited HF molecules and 2-D images of the population inversion between two adjacent excited states in chemically produced HF. In addition we presented data showing the capability of the AIRIS device to determine the spectral and spatial profiles of HF laser beams. This diagnositic device will be useful for a investigating a variety of parameters in the development of new, mid-IR chemical lasers.

Acknowledgments

The authors would like to thank Katie Boates of Mount Holyoke College for assistance in the image data reduction. We also gratefully acknowledge the Air Force Research Laboratory Directed Energy Directorate, Kirtland AFB, NM for support of the effort under Contract #F29601-01-C-0091.

References

1. Gross, R.W.F. and Bott, J.F., *Handbook of Chemical Lasers*, John Wiley & Sons, New York, 1976.
2. Kwok, M.A., "Measurement and Analysis of the HF Radiation form a Reacting Supersonic Jet", Technical Report TR-0074(4530)-3, The Aerospace Corporation, Los Angeles, CA (1973).
3. Sentman, L.H, "Mechanisms of HF Laser Performance," *XIII International Symposium on Gas Flow and Chemical Lasers and High-Power Laser Conference*, Vol. 4184, Invited paper, Proceedings, SPIE, Florence, Italy (September 2000).
4. Rapagnani, N.L. and Davis, S.J., "Laser Induced Fluorescence Measurements in a Chemical Laser Flowfield", *AIAA Journ.* **17**, p. 1402, 1979.
5. Rapagnani, N.L. and Davis, S.J., "Laser Induced Fluorescence: A Diagnostic for Fluid Mechanics," Lasers and Applications" IV-5, 127 (1985).
6. Jacquinot, P. and Dufour, C., *CRMS J.Resh.* **61**, p. 91, 1948.
7. Neumann, D.K., Clark, P.K., Shea, R.F., and Davis, S.J., "O_2 Pressure Broadening of the Iodine $^2P_{1/2}\rightarrow$ $^2P_{3/2}$ Transition", *J.Chem. Phys.* **79**, p. 4680, 1983.